Journal of Magnetic Resonance **137,** 295–310 (1999)
Article ID jmre.1998.1681, available online at http://www.idealibrary.com on IDEAL®

A Study of Dipolar Interactions and Dynamic Processes of Water Molecules in Tendon by ^{1}H and ^{2}H Homonuclear and Heteronuclear Multiple-Quantum-Filtered NMR Spectroscopy

Uzi Eliav and Gil Navon

School of Chemistry, Tel Aviv University, Ramat Aviv, Tel Aviv 69978, Israel

Received May 28, 1998; revised December 4, 1998

The effect of proton exchange on the measurement of ^{1}H–^{1}H, ^{1}H–^{2}H, and ^{2}H–^{2}H residual dipolar interactions in water molecules in bovine Achilles tendons was investigated using double-quantum-filtered (DQF) NMR and new pulse sequences based on heteronuclear and homonuclear multiple-quantum filtering (MQF). Derivation of theoretical expressions for these techniques allowed evaluation of the ^{1}H–^{1}H and ^{1}H–^{2}H residual dipolar interactions and the proton exchange rate at a temperature of 24°C and above, where no dipolar splitting is evident. The values obtained for these parameters at 24°C were 300 and 50 Hz and 3000 s^{-1}, respectively. The results for the residual dipolar interactions were verified by repeating the above measurements at a temperature of 1.5°C, where the spectra of the H_2O molecules were well resolved, so that the ^{1}H–^{1}H dipolar interaction could be determined directly from the observed splitting. Analysis of the MQF experiments at 1.5°C, where the proton exchange was in the intermediate regime for the ^{1}H–^{2}H dipolar interaction, confirmed the result obtained at 24°C for this interaction. A strong dependence of the intensities of the MQF signals on the proton exchange rate, in the intermediate and the fast exchange regimes, was observed and theoretically interpreted. This leads to the conclusion that the MQF techniques are mostly useful for tissues where the residual dipolar interaction is not significantly smaller than the proton exchange rate. Dependence of the relaxation times and signal intensities of the MQF experiments on the orientation of the tendon with respect to the magnetic field was observed and analyzed. One of the results of the theoretical analysis is that, in the fast exchange regime, the signal decay rates in the MQF experiments as well as in the spin echo or CPMG pulse sequences (T_2) depend on the orientation as the square of the second-rank Legendre polynomial.

Key Words: **dipolar interaction; proton–proton dipolar interaction; proton–deuteron dipolar interaction; deuteron–deuteron dipolar interaction; heteronuclear triple-quantum filter; homonuclear triple-quantum filter; proton–deuterium spin correlation.**

INTRODUCTION

T_2-weighted MRI of ordered biological tissues such as articular cartilage and tendon was found to be orientation dependent (*1, 2*). This orientation dependence results in an image that does not faithfully represent the chemical composition and structure, complicating the interpretation of the image. The T_2 orientation dependence was attributed in previous publications to a residual dipolar interaction which originates from the interaction of water molecules with fibrous proteins such as collagen (*3–7*). However, no interpretation of this orientation dependence, based on the modulation of the dipolar interaction by the dynamics of the water molecules, was given. In tissues, these studies were hampered by the interference of the signals coming from isotropic and anisotropic media. Water bound to fibrous proteins is an example of an anisotropic medium whereas free water or water bound to globular proteins, or to polysaccharides, is an example of isotropic media. With the advent of multiple-quantum-filtered (MQF) NMR techniques it has been demonstrated that filtering the NMR signal through $2I$ and $2I - 1$ coherence for even and odd spin nuclei, respectively, enables the observation of the contributions to the FID that originate exclusively from anisotropic media (*8–13*).

In a system of fibrous proteins and water, proton–proton dipolar interaction can be intramolecular (between protons of the protein, or the protons within the water molecules) as well as intermolecular (between the water and the protein protons). One way to distinguish between these types of interactions is to replace some of the H_2O molecules with D_2O and investigate the correlations between protons and deuterons created by dipolar interactions. Such correlation studies were made possible by recent studies of dipolar interactions between quadrupolar nuclei and protons, using multiple-quantum-filtering techniques. In these studies it has been shown that the $2I$ transitions are very sensitive to heteronuclear dipolar interactions. This was demonstrated for the triple-quantum transitions of the spin $I = \frac{3}{2}$ nuclei ^{7}Li and ^{23}Na (*14–16*). Furthermore, it has been shown theoretically that correlation between quadrupolar nuclei and each of the protons may be possible. Such techniques are used in the current work for the study of ^{1}H–^{2}H and ^{2}H–^{2}H correlations.

THEORY

Residual quadrupolar and dipolar interactions lead to the formation of high-rank tensors ($T_{l,\pm1}$, $l = 2, \ldots, 2I$) that can

1090-7807/99 $30.00

be detected by MQF (*8–16*). The residual interactions are the result of anisotropic motion in systems with either macroscopic or local order. In the first case, the directors have a unique spatial orientation while, in the second case, the orientations of the local directors are evenly distributed.

In order to identify the groups of nuclei that interact with each other, one may follow the correlations between their spin states. This is particularly true in systems where the NOE is negligible. In terms of the spherical tensors one should find a mechanism that transforms the tensors $T_{l,\pm p}$ of one nucleus to tensors that consist of the direct product of these tensors with those of another nucleus $T'_{l',\pm p'}$, i.e., $T_{l,\pm p} \times T'_{l',\pm p'}$. Provided that $T'_{l',\pm p'}$ are different from $T'_{0,0}$ the direct product tensors carry spectroscopic information characteristic of each of the nuclei, thereby making it possible to identify the nuclei that interact with each other. MQF techniques make it possible to remove, from the FID, any contribution that does not originate from the tensors $T_{l,\pm p} \times T'_{l',\pm p'}$.

In all the MQF methods to be described below, the tensors $T_{1,\pm 1}$ are first excited and then allowed to evolve under the effect of dipolar (or quadrupolar) interactions into tensors with ranks higher than one. Subsequently, tensors with coherences of interest are selected by a suitable phase cycling and then allowed to evolve into the detectable tensors $T_{1,\pm 1}$. In the case of protons, the above process is a result of dipolar interactions; i.e., the tensors $T_{1,\pm 1}$ evolve into $T_{2,\pm 1}$ which consist of the product of $T_{1,\pm 1}$ of one proton with $T_{1,0}$ of another proton. For quadrupolar nuclei, tensors such as $T_{2,\pm 1}$, which are formed under the influence of quadrupolar interactions, do not reflect any correlation with other nuclei. Furthermore, since the quadrupolar interaction is usually much larger than the dipolar interaction, the formation and the decay of these tensors are dominated by the former interaction and thus their dynamics cannot be used to study dipolar interactions. To overcome this difficulty one must consider tensors that are affected by quadrupolar interactions only to the second order. In previous works, we have shown that the dipolar interaction has a significant effect on the relaxation of the $|m\rangle \leftrightarrow |-m\rangle$ transitions of quadrupolar nuclei in isotropic media (*15, 16*) with the strongest effect obtained for $m = I$. For these transitions, the quadrupolar relaxation is determined by nonsecular terms while the relaxation due to the dipolar interaction is a result of secular terms. In anisotropic systems, one must consider the additional effects of the residual quadrupolar and dipolar interactions. While the first interaction does not have a first order effect on the time evolution of the $|m\rangle \leftrightarrow |-m\rangle$ transitions, the residual dipolar interaction does have such an effect.

There are a number of dynamic processes that result in the observed residual quadrupolar and dipolar interactions and relaxation times:

(a) Anisotropic reorientation of the water molecules bound to the protein, resulting in residual quadrupolar and dipolar interactions and relaxation effects. The time scale of this motion is typically 10^{-10}–10^{-7} s.

(b) Fast isotropic reorientation of water molecules in the bulk where the time scale is shorter than 10^{-10} s. This motion yields no residual quadrupolar and dipolar interactions and a very small contribution to relaxation.

(c) Fast chemical exchange between bound and free water molecules with a time scale shorter than 10^{-9} s (*17*). This process scales down the residual quadrupolar and dipolar interactions and the relaxation rates from their values in the bound states. For cases in which the chemical exchange is faster than the reorientation of the bound water molecules it will act in a fashion similar to that of isotropic motion, further scaling down the residual interactions in the bound state.

(d) Proton exchange between water molecules. The time scale of this process in the bulk is, depending on the temperature and pH, between 10^{-4} and 10^{-2} s. The proton exchange is expected to alter the spins states and thus interchanges between the peaks that are a result of the residual dipolar interaction. Specifically, the wavefunction of a given water molecule which is either $|m\alpha_a\rangle$ or $|m\beta_a\rangle$ changes to either $|m\beta_b\rangle$ or $|m\alpha_b\rangle$, respectively. m ($m = \alpha, \beta$) is the spin state of the nuclei in the water molecule while α_a and β_a are the spin states of the other proton in the water molecule before it interchanged, and β_b and α_b are the spin states of the other proton after the interchange has occurred. A detailed discussion of the kinetics and their effect on the spectra can be found in the Appendix.

In contrast to residual dipolar interaction, residual quadrupolar interaction is not expected to be significantly affected by proton exchange. Discussion of the effect of the latter interaction on the MQF spectra was given previously (*8, 9, 11–13, 18*).

For the system of the current study, three types of dipolar interactions are of interest: ^{1}H–^{1}H, ^{1}H–^{2}H, and ^{2}H–^{2}H. On the basis of the above discussion, the effect of the residual part of each of these interactions should be considered under two types of conditions. One occurs when the proton exchange is very slow, and the other when proton exchange is very effective. The theoretical section is divided into five sections; the first four discuss the three types of residual dipolar interactions, while the fifth summarizes the relaxation effects. Within each of the first four sections, we discuss the NMR signals with and without dynamic effects and present methods for their measurement.

a. The Effect of ^{1}H–^{1}H Residual Dipolar Interaction on the Single-Quantum Tensors of the ^{1}H Nucleus

I. Without the Effect of Hydrogen Exchange

The single-quantum transitions of a pair of protons can be described, as a first approximation, as those of an effective spin 1. The secular terms are the only terms with a first-order effect

on the spherical tensors. Thus the normalized $T_{1,\pm1}$ and $T_{2,\pm1}$ are sufficient for describing their dynamics. Given the initial condition for the density matrix, $\rho(0) = T_{1,\pm1}\rho_{T_{1,\pm1}} + T_{2,\pm1}\rho_{T_{2,\pm1}}$, the density matrix at some time later, t, is $\rho(t) = U\rho(0)$, where U is given by (see Appendix)

$$U = \begin{pmatrix} & T_{1,\pm1} & T_{2,\pm1} \\ & \cos\tfrac{3}{2}\omega_{^1\mathrm{H}-^1\mathrm{H}}t & \mp i\sin\tfrac{3}{2}\omega_{^1\mathrm{H}-^1\mathrm{H}}t \\ & \mp i\sin\tfrac{3}{2}\omega_{^1\mathrm{H}-^1\mathrm{H}}t & \cos\tfrac{3}{2}\omega_{^1\mathrm{H}-^1\mathrm{H}}t \end{pmatrix}, \quad [1]$$

with

$$\omega_{^1\mathrm{H}-^1\mathrm{H}} = \omega^{\mathrm{loc}}_{^1\mathrm{H}-^1\mathrm{H}}(3\cos^2\theta - 1)/2 = \frac{fS\hbar^2\gamma^2_{^1\mathrm{H}}}{2r^3_{^1\mathrm{H}-^1\mathrm{H}}}(3\cos^2\theta - 1), \quad [2]$$

where $\omega_{^1\mathrm{H}-^1\mathrm{H}}$ is the proton–proton residual dipolar interaction, θ the angle between the director of reorientation and the magnetic field, S the order parameter, and f the fraction of bound nuclei.

As can be seen from the off-diagonal element of U (Eq. [1]), the tensors $T_{2,\pm1}$ can evolve from $T_{1,\pm1}$ according to $i\sin\frac{3}{2}\omega_{^1\mathrm{H}-^1\mathrm{H}}t$. Thus, in experiments such as conventional DQF (*19*), where this element of U determines the FID, the spectrum consists of two lines in antiphase to each other (i.e., the Fourier transform of $\sin\frac{3}{2}\omega_{^1\mathrm{H}-^1\mathrm{H}}t$).

II. The Dynamic Effect: Modulation of ^{1}H–^{1}H Residual Dipolar Interaction by Spin Exchange

On the basis of the above model it is shown in the Appendix that the evolution of the normalized spin operators $T_{1,\pm1}$ and $T_{2,\pm1}$ is given by the matrix U,

$$U = \begin{pmatrix} T^{\mathrm{a}}_{1,\pm1} & T^{\mathrm{b}}_{1,\pm1} & T^{\mathrm{a}}_{2,\pm1} & T^{\mathrm{b}}_{2,\pm1} \\ U_1 & U_2 & U_3 & 0 \\ U_2 & U_1 & 0 & U_3 \\ U_3 & 0 & U_1 & U_2 \\ 0 & U_3 & U_2 & U_1 \end{pmatrix}, \quad [3]$$

where a and b represent the protons that were interchanged and U_1, U_2, and U_3 are given by the following:

for $k < \delta$,

$$U_1(t) = e^{-kt/2}\cos rt, \quad U_2(t) = \frac{k}{2r}e^{-kt/2}\sin rt$$

$$U_3(t) = \mp i\frac{\delta}{2r}e^{-kt/2}\sin rt, \quad [3a]$$

where the $\mp$ corresponds to the sign of the single-quantum coherence;

for $k = \delta$,

$$U_1(t) = e^{-\delta t/2}, \quad U_2(t) = \frac{k}{2}e^{-\delta t/2}t$$

$$U_3(t) = \mp i\frac{\delta}{2}e^{-\delta t/2}t; \quad [3b]$$

for $k > \delta$,

$$U_1(t) = e^{-kt/2}\cosh\rho t, \quad U_2(t) = \frac{k}{2\rho}e^{-kt/2}\sinh\rho t$$

$$U_3(t) = \mp i\frac{\delta}{2\rho}e^{-kt/2}\sinh\rho t \quad [3c]$$

$$\rho = \frac{\sqrt{k^2-\delta^2}}{2}, \quad r = \frac{\sqrt{\delta^2-k^2}}{2}, \quad \delta = 3\omega_{^1\mathrm{H}-^1\mathrm{H}}.$$

The rate of proton exchange is given by k. As can be seen from Eq. [3], in the limit of $k = 0$, it reduces to

$$U_1 = \cos\tfrac{3}{2}\omega_{^1\mathrm{H}-^1\mathrm{H}}t, \quad U_2 = 0, \quad U_3 = \mp i\sin\tfrac{3}{2}\omega_{^1\mathrm{H}-^1\mathrm{H}}t, \quad [4]$$

where a well-resolved spectrum with splitting of $3\omega_{^1\mathrm{H}-^1\mathrm{H}}$ is observed and the second-rank tensors, $T_{2,\pm1}$, evolve according to U_3. As can be seen from Eq. [3] under the condition $k > 3\omega_{^1\mathrm{H}-^1\mathrm{H}}$, a coalescence occurs and the time dependence of the elements of U is biexponential. Thus, the Fourier transformation of the elements of U consists of a superposition of two Lorentzian lines of different widths. For the element U_1, the two lines have the same phase while for U_2 and U_3 they are in antiphase to one another. The widths of these two lines depend on ρ (Eq. [3c]) and thus are expected to change with the orientation of the samples relative to the magnetic field. Another situation, which is common in biological tissues, is $k \gg 3\omega_{^1\mathrm{H}-^1\mathrm{H}}$. For this condition one obtains from Eq. [3c], for the decay of the transverse magnetization, $T_{1,\pm1} = T^{\mathrm{a}}_{1,\pm1} + T^{\mathrm{b}}_{1,\pm1}$, given by the sum of the elements U_1 and U_2, a monoexponential decay:

$$U_1 + U_2 = \exp\left(-\frac{1}{4}\frac{\delta^2}{k}t\right), \quad \delta = 3\omega_{^1\mathrm{H}-^1\mathrm{H}}. \quad [5]$$

Thus one can write

$$\frac{1}{T_2} = \frac{1}{4}\frac{\delta^2}{k}. \quad [6]$$

The expression in Eq. [6] clearly shows that $1/T_2$ is orientation dependent, a fact that has been shown by measurements such as a single spin echo and CPMG pulse sequences of articular cartilage and tendon (*1–7*). Deviations from the predicted

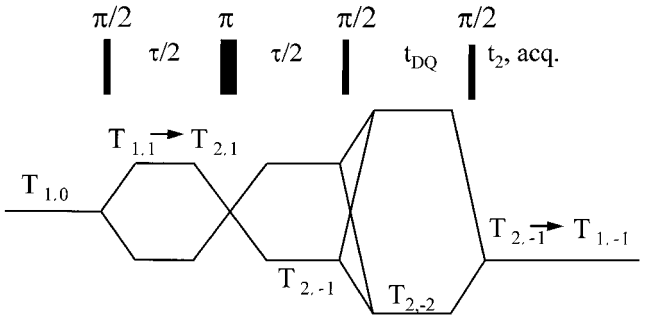

FIG. 1. The pulse sequence and the coherence pathway of the conventional DQF experiment. The given pathway is selected by the appropriate phase cycling (*8*, *9*).

dependence of $1/T_2$ on $(3\cos^2\theta - 1)^2$ (Eqs. [5], [6], and [2]) may be observed in the experiments due to several factors, e.g., an exchange rate which may not be sufficiently larger than δ, limiting the validity of Eq. [6], a distribution of the orientation of macromolecules with respect to the magnetic field, and contributions to the relaxation from isotropic compartments. In the extreme limit of very large k, $U_1 = U_2 = 1$ and $U_3 = 0$, making the evolution of the tensors $T_{2,\pm1}$ from $T_{1,\pm1}$ impossible.

III. Pulse Sequences for the Measurement of the Residual ^1H–^1H Interaction

As was shown in Sections a.I and a.II residual dipolar interaction leads to the formation of the tensors $T_{2,\pm1}$ from $T_{1,\pm1}$. Thus, by measuring the rate of formation of $T_{2,\pm1}$, one can extract the value of ^1H–^1H residual dipolar interaction. The pulse sequence suitable for this purpose is the standard double-quantum filtration (DQF) shown, along with the coherence pathway and the relevant spherical tensors for each time interval, in Fig. 1. In principle, pulse sequences such as spin echo and single-pulse experiments could serve the same purpose. However, in many biological systems, signals that stem from compartments with an anisotropic environment are masked by much stronger signals that originate from an isotropic environment. DQF methods suppress these strong signals, due to the fact that they detect the tensors $T_{2,\pm1}$ that are not formed in isotropic media. On the basis of expressions for U_3 in Eq. [3], one obtains the following expression for the FID of the DQF experiment:

$$\text{FID} \propto U_3(\tau)U_3(t_2); \qquad [7]$$

for $k < \delta$,

$$\text{FID} \propto \frac{\delta^2}{r^2}\, e^{-k\tau/2}\sin r\tau e^{-kt_2/2}\sin rt_2; \qquad [7a]$$

for $k = \delta$,

$$\text{FID} \propto \delta^2\, e^{-\delta\tau/2}\tau e^{-\delta t_2/2}t_2; \qquad [7b]$$

for $k > \delta$,

$$\text{FID} \propto \frac{\delta^2}{\rho^2}\, e^{-k\tau/2}\sinh \rho\tau e^{-kt_2/2}\sinh \rho t_2$$

$$\rho = \frac{\sqrt{k^2 - \delta^2}}{2}, \quad r = \frac{\sqrt{\delta^2 - k^2}}{2}, \quad \delta = 3\omega_{^1\text{H}-^1\text{H}} \qquad [7c]$$

In the limit of $k = 0$, the expression in Eq. [7a] reduces to

$$\text{FID} \propto \sin \tfrac{3}{2}\omega_{^1\text{H}-^1\text{H}}\tau \sin \tfrac{3}{2}\omega_{^1\text{H}-^1\text{H}}t_2. \qquad [8]$$

As expected, this expression is similar to that obtained previously (*8*, *13*) for the conventional DQF experiment of $I = 1$. The spectra obtained by Fourier transformation of the expression in Eq. [7] consists of two peaks in antiphase to each other.

Under the condition $k > 3\omega_{^1\text{H}-^1\text{H}}$, the time dependence of the FID is biexponential with decay rates which are orientation dependent, as expected from Eq. [7c]. For τ and $t_2 > 1/k$ and $k \gg 3\omega_{^1\text{H}-^1\text{H}}$ the expression in Eq. [7c] for the FID simplifies to

$$\text{FID} \propto \left(\frac{\delta}{k}\right)^2 e^{-\tau/T_2}e^{-t_2/T_2}, \qquad [9]$$

where $1/T_2$ is defined in Eq. [6]. As seen from Eq. [9], the FID is dependent on the orientation as $\omega^2_{^1\text{H}-^1\text{H}}$. Thus for cases with large $\omega^2_{^1\text{H}-^1\text{H}}$, where T_2 is short and the SQ peak intensity is low, the DQF signal is large. The converse is also true. For small $\omega_{^1\text{H}-^1\text{H}}$, as is the case for the magic angle orientation ($\theta = 54.7°$), the DQF signal vanishes. Another important characteristic of the DQF spectra under the condition $k \gg 3\omega_{^1\text{H}-^1\text{H}}$ is the reduction of the intensity in proportion to $1/k^2$. This dependence makes this experiment very sensitive to conditions that affect the proton exchange rate. It is clear that in the limit of very fast exchange rate no DQF signal can be observed.

An alternative method to the conventional DQF pulse sequence, where the peaks are in antiphase to one another, is the DQF pulse sequence given in Fig. 2 and denoted as in-phase DQF (IP-DQF) (*20*). The spectrum obtained by IP-DQF represents peaks that have the same phase. On the basis of the evolution matrix given in Eq. [3] the following expression is obtained for the FID measured by the IP-DQF pulse sequence:

$$\text{FID} \propto U_3^2(\tau/2)[U_1(t_2) + U_2(t_2)]. \qquad [10]$$

The dependence of the FID given in Eq. [10] on the orientation

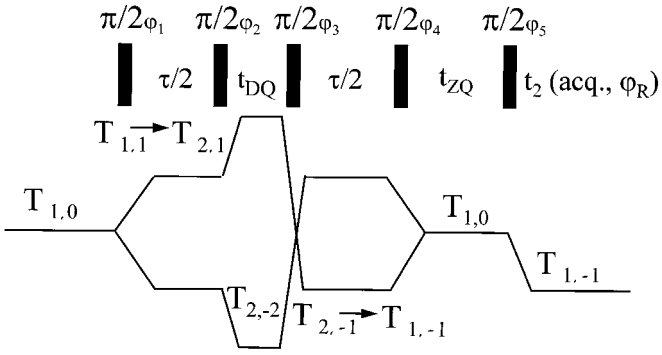

FIG. 2. The IP-DQF pulse sequence. It consists of a double-quantum filter followed by a zero-quantum filter (*20*). A phase cycling of 64 steps was used: $\varphi_1 = j*\pi/2 + k*0 + m*0$, $\varphi_2 = j*\pi/2 + k*\pi/2 + m*0$, $\varphi_3 = j*0 + k*\pi/2 + m*\pi/2$, $\varphi_4 = j*0 + k*0 + m*\pi/2$, $\varphi_5 = 64*0$, $\varphi_R = (j + k + m)*\pi$ (j, k, m = 0, 1, 2, 3). The asterisk denotes multiplication.

and the proton exchange rate is similar to that of the conventional DQF (Eq. [7]) and thus need not be discussed further.

^{1}H–^{2}H residual dipolar interaction. The ^{1}H–^{2}H dipolar interaction can be studied by investigating either the ^{1}H or the ^{2}H nuclei. In both cases, the homonuclear ^{1}H–^{1}H and ^{2}H–^{2}H dipolar interactions affect the dynamics of the spin states of the ^{1}H and ^{2}H nuclei, respectively. The effect of the dipolar interaction on the transverse magnetization of the protons is larger than that on the longitudinal magnetization. Therefore only the effect on the $T_{1,\pm1}$ tensors of the protons will be studied. For the deuterons, as discussed above, the effect of the dipolar interaction is most pronounced on the DQ transitions, i.e., the $T_{2,\pm2}$ tensors.

b. The Effect of ^{1}H–^{2}H Residual Dipolar Interaction on the $T_{1,\pm1}$ Tensors of the ^{1}H Nucleus

I. Without the Effect of Hydrogen Exchange

The ^{1}H–^{2}H dipolar interaction has a first-order effect on the $T_{1,\pm1}$ (^{1}H) tensors giving correlations with $T_{1,0}$(^{2}H) and $T_{2,0}$(^{2}H). In analogy to the formalism which was used to obtain the effect of ^{1}H–^{1}H residual dipolar interaction, the following evolution matrix is obtained (for details see the Appendix),

$$U = \begin{array}{c} \begin{matrix} \frac{1}{\sqrt{3}}T_{1,\pm1}(^1\mathrm{H}) & T_{1,\pm1}(^1\mathrm{H})T_{1,0}(^2\mathrm{H}) & T_{1,\pm1}(^1\mathrm{H})T_{2,0}(^2\mathrm{H}) \end{matrix} \\ \begin{pmatrix} \frac{1}{3}(1+2\cos 2\omega_{^1\mathrm{H}-^2\mathrm{H}}t) & \mp i\sqrt{\frac{2}{3}}\sin 2\omega_{^1\mathrm{H}-^2\mathrm{H}}t & -\frac{\sqrt{2}}{3}(1-\cos 2\omega_{^1\mathrm{H}-^2\mathrm{H}}t) \\ \mp i\sqrt{\frac{2}{3}}\sin 2\omega_{^1\mathrm{H}-^2\mathrm{H}}t & \cos 2\omega_{^1\mathrm{H}-^2\mathrm{H}}t & \mp i\frac{\sqrt{3}}{3}\sin 2\omega_{^1\mathrm{H}-^2\mathrm{H}}t \\ -\frac{\sqrt{2}}{3}(1-\cos 2\omega_{^1\mathrm{H}-^2\mathrm{H}}t) & \mp i\frac{\sqrt{2}}{3}\sin 2\omega_{^1\mathrm{H}-^2\mathrm{H}}t & \frac{1}{3}(2+\cos 2\omega_{^1\mathrm{H}-^2\mathrm{H}}t) \end{pmatrix} \end{array}, \qquad [11]$$

with $\omega_{^1\mathrm{H}-^2\mathrm{H}} = \omega^{\mathrm{loc}}_{^1\mathrm{H}-^2\mathrm{H}}(3\cos^2\theta - 1)/2$, where $\omega^{\mathrm{loc}}_{^1\mathrm{H}-^2\mathrm{H}} = fS\hbar^2\gamma_{^1\mathrm{H}}\gamma_{^2\mathrm{H}}/r^3_{^1\mathrm{H}-^2\mathrm{H}}$, and S is the order parameter, f the fraction of bound nuclei, and θ the angle between the director of reorientation and the magnetic field. The Fourier transforms of the diagonal element, $U_{1,1}$, gives three lines with equal intensities as expected in experiments with a single 90° pulse. The off-diagonal element $U_{1,2}$ (Eq. [11]) describes the formation of the tensors $T_{1,\pm1}(^1\mathrm{H})T_{1,0}(^2\mathrm{H})$ from $T_{1,\pm1}(^1\mathrm{H})$. Their Fourier transforms consist of the two outermost lines of the single-pulse experiments, in antiphase to one another. The off-diagonal element $U_{1,3}$ (Eq. [11]) describes the formation of the tensors $T_{1,\pm1}(^1\mathrm{H})T_{2,0}(^2\mathrm{H})$ from $T_{1,\pm1}(^1\mathrm{H})$. Their Fourier transforms consist of three lines with an intensity ratio of $-1{:}2{:}-1$.

II. Pulse Sequences for the Measurement of the Effect of the Residual ^{1}H–^{2}H Interaction on the $T_{1,\pm1}(^1\mathrm{H})$ Tensors of Protons

The pulse sequence shown in Fig. 3 detects the formation of either the tensors $T_{1,\pm1}(^1\mathrm{H})T_{1,0}(^2\mathrm{H})$ or $T_{1,\pm1}(^1\mathrm{H})T_{2,0}(^2\mathrm{H})$ which transform into $T_{1,\pm1}(^1\mathrm{H})T_{1,\pm1}(^2\mathrm{H})$ or $T_{1,\pm1}(^1\mathrm{H})T_{2,\pm2}(^2\mathrm{H})$, respectively, by selecting the appropriate phase cycling and pulse widths of the last two pulses on the deuterons. The two selections of the phase cycling will be denoted as Inv-XSQ and Inv-XDQ, respectively.

c. The Effect of ^{1}H–X Residual Dipolar Interaction on the $T_{2I,p}$ Tensors of the X Nucleus

I. Without the Effect of Hydrogen Exchange

It is shown in the Appendix that the effect of the residual dipolar interaction between a quadrupolar nucleus and a proton on the $|m\rangle \leftrightarrow |-m\rangle$ transitions is given by the evolution matrix

$$U = \begin{array}{c} \begin{matrix} \frac{1}{\sqrt{2}}T_{2I,p}(\mathrm{X}) & T_{2I,p}(\mathrm{X})T_{1,0}(^1\mathrm{H}) \end{matrix} \\ \begin{pmatrix} \cos p\omega_{^1\mathrm{H}-\mathrm{X}}t & -i\sin p\omega_{^1\mathrm{H}-\mathrm{X}}t \\ -i\sin p\omega_{^1\mathrm{H}-\mathrm{X}}t & \cos p\omega_{^1\mathrm{H}-\mathrm{X}}t \end{pmatrix} \end{array}, \qquad [12]$$

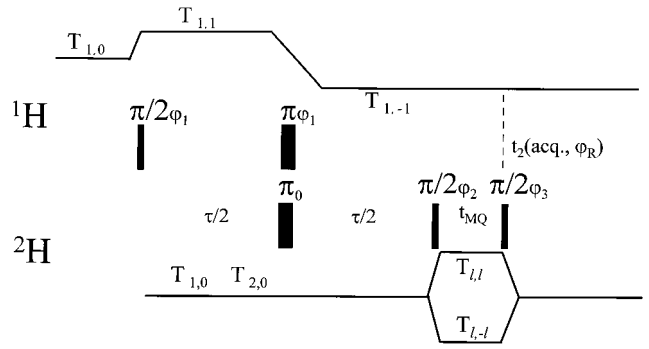

FIG. 3. Proton-detected pulse sequences with a SQ or DQ filters for the X nucleus (Inv-SQX or Inv-DQX, respectively). A phase cycling of 16 or 64 steps was used for the Inv-SQX ($l = 1$) and Inv-DQX ($l = 2$) pulse sequences, respectively: $\varphi_1 = j*\pi + k*0 + m*0$, $\varphi_2 = j*0 + k*\pi/l + m*0$, $\varphi_3 = j*0 + k*0 + m*\pi/l$, $\varphi_R = j*\pi/2 + (k + m)*\pi/l$, $j = 0, 1, 2, 3$ and $k, m = 0, \ldots, 2l - 1$. The asterisk denotes multiplication.

where $p = \pm 2m$ ($m = \frac{1}{2}, \ldots, I$ or $m = 1, \ldots, I$ for half-integer or integer spins, respectively). As seen from Eq. [12], the Fourier transformation of the diagonal elements yields two peaks with the same phase, separated by $2p\omega_{^1H-X}$. The off-diagonal elements describe the formation of the correlation tensors $T_{2I,p}(X)T_{1,0}(^1H)$ from $T_{2I,p}(X)$. The Fourier transformation of the off-diagonal elements yields two peaks with opposite phases and also separated by $2p\omega_{^1H-X}$. Selecting deuterium as the X nucleus $I = 1$, $p = \pm 2$, and the splitting is $4\omega_{^1H-^2H}$. The ratio between this splitting and that obtained from the DQF experiments (Section a.III) in systems with ^1H–^1H dipolar interaction is $4\gamma_{^2H}/3\gamma_{^1H} = 0.205$.

II. The Dynamic Effect: Modulation of ^1H–^2H Residual Dipolar Interaction by Spin Exchange

The effect of proton exchange on the tensors $T_{2,\pm 2}$ of the deuterons was calculated using the same dynamic model given in Section a.I for the effect of proton exchange on the spectrum of protons coupled by ^1H–^1H dipolar interaction (Eq. [3]). The details of the calculations are given in the Appendix with the result presented in the equation

Due to the mathematical similarity of the equations leading to Eqs. [3] and [13] the expressions for U_1, U_2, and U_3 can be obtained from Eq. [3] by replacing the expression for δ with

$$\delta = 4\omega_{^1H-^2H}. \qquad [14]$$

Similar to Eq. [3], Eq. [13] consists of three equations for the cases $k < \delta$, $k = \delta$, and $k > \delta$. They are denoted as [13a] through [13c]. In analogy to the case of proton–proton interaction in the limit of $k = 0$, the spectra due to the diagonal elements are well resolved, while for very fast exchange ($k \rightarrow \infty$) full coalescence is obtained. As for the off-diagonal elements, they have their maximum value when $k = 0$ and diminish to zero as $k \rightarrow \infty$. The case of proton–deuteron interaction under the condition $k \gg 4\omega_{^1H-^2H}$ is of interest in the current study of biological tissues. The results can be obtained from Eqs. [5], [6], and [9] by replacing $\delta = 3\omega_{^1H-^1H}$ with $\delta = 4\omega_{^1H-^2H}$. Clearly, also in the current case, the rates of decay of the elements of the matrix U are dependent on the orientation as $\omega^2_{^1H-^2H}$.

III. Pulse Sequences for the Measurement of the Effect of the Residual ^1H–^2H Interaction on the Double-Quantum Transition of Deuterons

Two types of experiments were carried out. The first (Fig. 4) measures the diagonal element of the matrix $U\dagger U$ (U is given in Eqs. [12] and [13]; $U\dagger$ is its Hermitian conjugate) that describes the time dependence of the tensors $T_{2,\pm 2}$. It is denoted as double-quantum relaxation with an echo (DQRE). The second pulse sequence (Fig. 5), denoted as heteronuclear triple-quantum filter (Het-TQF), measures the off-diagonal elements of U (Eqs. [12] and [13]). It can be used to identify the protons that correlate with the deuterons.

In the calculation of the FID of the DQRE and Het-TQF pulse sequences, one can assume that at the beginning of the t_{DQ} period only the tensors $T_{2,\pm 2}(^2H)$ have to be considered and the tensors $T_{2,\pm 2}(^2H)T_{1,0}(^1H)$ (which also represent double-quantum coherence for ^2H) can be ignored. This approximation is justified for the following reason: the third-rank tensors $T_{2,\pm 2}(^2H)T_{1,0}(^1H)$ which originate from the tensors $T_{2,\pm 1}(^2H)T_{1,0}(^1H)$ may be formed during the creation time τ.

$$U = \begin{array}{c} \begin{array}{cccc} \frac{1}{\sqrt{2}}T_{2,\pm 2}(^2H) & \frac{1}{\sqrt{2}}T_{2,\pm 2}(^2H) & T_{2,\pm 2}(^2H)T^a_{1,0}(^1H) & T_{2,\pm 21}(^2H)T^b_{1,0}(^1H) \end{array} \\ \left(\begin{array}{cccc} U_1 & U_2 & U_3 & 0 \\ U_2 & U_1 & 0 & U_3 \\ U_3 & 0 & U_1 & U_2 \\ 0 & U_3 & U_2 & U_1 \end{array} \right) \end{array}. \qquad [13]$$

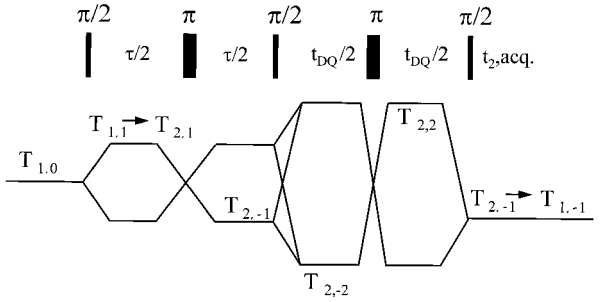

FIG. 4. A pulse sequence designed to measure the double-quantum relaxation time, T_{DQ} (DQRE). The phase cycling is identical to that of the conventional DQF sequence (*8*, *9*).

However, the formation of these tensors in most practical cases is much slower than the decay of the tensors $T_{2,\pm1}(^2\mathrm{H})$ by quadrupolar interaction and thus can be neglected. The same consideration leads to the conclusion that any formation of the tensor $T_{2,-1}(^2\mathrm{H})$ and subsequently the observable tensor $T_{1,-1}(^2\mathrm{H})$ from $T_{2,-1}(^2\mathrm{H})T_{1,0}(^1\mathrm{H})$ during the period t_2 can be neglected because it is too slow.

Thus, for the FID measured by the DQRE pulse sequence one obtains the following expressions:

for $k < 4\omega_{^1\mathrm{H}-^2\mathrm{H}}$

$$\mathrm{FID} \propto f_{12}^{q}(\tau, t_2)e^{-kt_{DQ}/2}\left[1 + \frac{k}{2r}\sin rt_{DQ} + \frac{k^2}{2r^2}\sin^2 r\,\frac{t_{DQ}}{2}\right] \qquad [15a]$$

which for $k \ll 4\omega_{^1\mathrm{H}-^2\mathrm{H}}$simplifies to

$$\mathrm{FID} \propto f_{12}^{q}(\tau, t_2)e^{-kt_{DQ}/2};$$

for $k = 4\omega_{^1\mathrm{H}-^2\mathrm{H}}$

$$\mathrm{FID} \propto f_{12}^{q}(\tau, t_2)e^{-2\omega_{^1\mathrm{H}-^2\mathrm{H}}t_{DQ}}[1 + 2\omega_{^1\mathrm{H}-^2\mathrm{H}}t_{DQ} + 2\omega^2_{^1\mathrm{H}-^2\mathrm{H}}t^2_{DQ}]; \qquad [15b]$$

for $k > 4\omega_{^1\mathrm{H}-^2\mathrm{H}}$

$$\mathrm{FID} \propto f_{12}^{q}(\tau, t_2)e^{-kt_{DQ}/2}\left[1 + \frac{k}{2\rho}\sinh \rho t_{DQ} + \frac{k^2}{2\rho^2}\sinh^2\rho\,\frac{t_{DQ}}{2}\right] \qquad [15c]$$

which for $k > 16\omega_{^1\mathrm{H}-^2\mathrm{H}}$ simplifies to

$$\mathrm{FID} \propto f_{12}^{q}(\tau, t_2)e^{-t_{DQ}/T_{DQ}}, \quad \frac{1}{T_{DQ}} = \frac{4\omega^2_{^1\mathrm{H}-^2\mathrm{H}}}{k}$$

$$\rho = \frac{\sqrt{k^2 - 16\omega^2_{^1\mathrm{H}-^2\mathrm{H}}}}{2}, \quad r = \frac{\sqrt{16\omega^2_{^1\mathrm{H}-^2\mathrm{H}} - k^2}}{2}.$$

$f_{12}^{q}(\tau, t_2)$ describes the spin dynamics during the periods τ and t_2. As stated above, during these periods the motion of the spins of the deuterons is dominated by the residual quadrupolar interaction, ω_Q, and under the additional condition $\omega_Q \gg k$, the function $f_{12}^{q}(\tau, t_2)$ can be approximated (*13*) by

$$f_{12}^{q}(\tau, t_2) = e^{-\tau/T_2}e^{-t_2/T_2}\sin \omega_Q\tau \sin \omega_Q t_2. \qquad [16]$$

In the limit of $k \gg 4\omega_{^1\mathrm{H}-^2\mathrm{H}}$ (in practice $k \geq 4\delta = 16\omega_{^1\mathrm{H}-^2\mathrm{H}}$ is sufficient), the relaxation rate of the double-quantum transition, $1/T_{DQ}$, is dependent on the orientation of the samples relative to the magnetic field like the relaxation rate $1/T_2$ (Eq. [6]), resulting from the proton–proton interaction. Clearly the same reasons that may cause $1/T_2$ to deviate from the expected orientation dependence (Eqs. [6] and [2]) apply for $1/T_{DQ}$. It is worth noting that Eq. [15a] predicts a full refocusing in the absence of spin exchange (the limit $k = 0$).

On the basis of Eq. [13] the following expressions are obtained for the Het-TQF experiment:

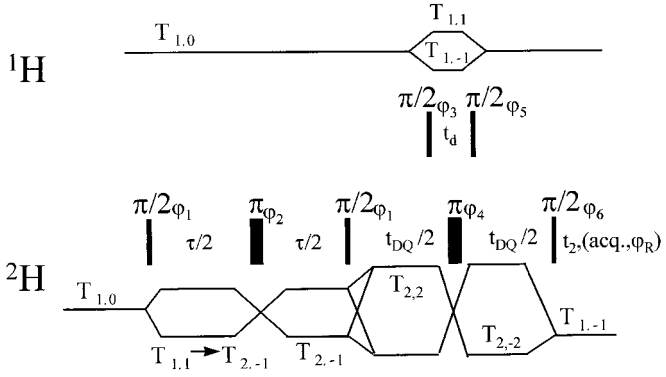

FIG. 5. A pulse sequence designed for the detection of heteronuclear third-rank tensors, denoted as heteronuclear triple-quantum filter (Het-TQF). Two kinds of phase cycling are implemented. One enables the detection of the two heteronuclear tensors $T_{3,\pm1}$ and $T_{3,\pm3}$, while the other selects only the heteronuclear triple-quantum tensors $T_{3,\pm3}$. The first type of phase cycling is $\varphi_1 = j*\pi/2 + k*0 + m*0$, $\varphi_2 = \varphi_1 + \pi/2$, $\varphi_3 = j*0 + k*\pi + m*0$, $\varphi_4 = \varphi_1$, $\varphi_5 = j*0 + k*\pi + m*\pi$, $\varphi_6 = 0$, $\varphi_R = (j + k + m)*\pi$, $j = 0, 1, 2, 3$ and $k, m = 0, 1$. In the second type of phase cycling φ_1, φ_2, and φ_6 are the same as for the first phase cycling but $\varphi_3 = \varphi_4 = j*0 + n*\pi/5$, $\varphi_5 = 0$, and $\varphi_R = (j + n)*\pi$, where $n = 0, 1, \ldots, 9$. The asterisk denotes multiplication. The time interval t_d is selected to be short enough so that relaxation effects were negligible.

$$\text{FID} \propto U_3^2(t_{DQ}/2)\, f_{12}^{q}(\tau, t_2); \qquad [17]$$

for $k < 4\omega_{^1H-^2H}$

$$\text{FID} \propto \frac{4\omega_{^1H-^2H}^2}{r^2} f_{12}^{q}(\tau, t_2) e^{-kt_{DQ}/2} \sin^2 \frac{rt_{DQ}}{2}; \qquad [17a]$$

for $k = 4\omega_{^1H-^2H}$

$$\text{FID} \propto \omega_{^1H-^2H}^2 f_{12}^{q}(\tau, t_2) e^{-2\omega_{^1H-^2H} t_{DQ}} t_{DQ}^2; \qquad [17b]$$

for $k > 4\omega_{^1H-^2H}$

$$\text{FID} \propto \frac{4\omega_{^1H-^2H}^2}{\rho^2} f_{12}^{q}(\tau, t_2) e^{-kt_{DQ}/2} \sinh^2 \frac{\rho t_{DQ}}{2}, \qquad [17c]$$

where ρ and r are given in Eq. [15] and $f_{12}^{q}(\tau, t_2)$ is presented in Eq. [16]. At the end of the τ period $T_{2,\pm1}(^2H)$ are formed and converted to $T_{2,\pm2}(^2H)$ by the 90° pulse (*8, 13, 18*). During the first $t_{DQ}/2$ period, as a result of the ^1H–^2H dipolar interaction, $T_{2,\pm2}(^2H)$ evolve into $T_{3,\pm2} = T_{2,\pm2}(^2H)T_{1,0}(^1H)$ while, during the second $t_{DQ}/2$ period, the reverse process takes place. By a suitable phase cycling of the two $\pi/2$ pulses on the ^1H nucleus, one selects the pathway (shown in Fig. 5) that allows the return of the tensors $T_{3,\pm2}$ either via $T_{3,\pm1} = T_{2,\pm2}(^2H)T_{1,\mp1}(^1H)$ and $T_{3,\pm3} = T_{2,\pm2}(^2H)T_{1,\pm1}(^1H)$ or, using another phase cycling, via the latter tensors. For both phase cyclings, the tensors $T_{2,\pm2}(^2H)$ are eliminated. Thus the FID is a result of the formation of the $T_{3,\pm2}$ tensors. Similar to the pulse sequences given in Figs. 1 and 3, in the limit of very fast exchange, the FID reduces to zero. It is worth noting that in the limit of $k = 0$ (i.e., no hydrogen exchange), Eq. [15] simplifies to the expression

$$\text{FID} \propto \sin \omega_Q\tau \sin^2 2\omega_{^1H-^2H} t_{DQ} \sin \omega_Q t_2. \qquad [18]$$

By selecting a constant value for t_{DQ} and varying the time interval, t_d, while decoupling the protons, it is possible to obtain a 2D map. One axis represents the ^2H spectrum, which is governed by the quadrupolar interaction, while the other axis represents the spectrum of those protons that are coupled to the deuterons and is governed by the ^1H–^1H dipolar interaction.

d. The Effect of ^2H–^2H Residual Dipolar Interaction on the $T_{2,\pm2}$ Tensors of Deuterium

Pulse Sequences for the Measurement of the Effect of the Residual ^2H–^2H Interaction on the $T_{2,\pm2}$ Tensors of Deuterons

The effect of the residual ^2H–^2H dipolar interaction on the double-quantum transitions in the absence of hydrogen exchange was given in a previous publication (*21*). A pulse sequence that detects the third-rank tensors created by the residual ^2H–^2H dipolar interaction is given in Fig. 6. In the following sections, we denote this sequence as homonuclear triple-quantum filter (Hom-TQF). Similar to the Het-TQF pulse sequence, one can assume that at the beginning of the first $t_{DQ}/2$ period only the tensors $T_{2,\pm2}(^2H)$ have to be considered. Subsequently these tensors evolve into $T_{3,\pm2}^{\pm2,0} = T_{2,\pm2}(^2H_1)T_{1,0}(^2H_2)$, $T_{4,\pm2}^{\pm2,0} = T_{2,\pm2}(^2H_1)T_{2,0}(^2H_2)$, and other double-quantum tensor operators which are a direct product of single-quantum tensors. The relaxation of ^2H single-quantum operators and their direct products are dominated by the quadrupolar interaction and thus for sufficiently long t_{DQ} can be ignored (*13, 15, 16, 18, 21*) and only $T_{3,\pm2}^{\pm2,0}$ and $T_{4,\pm2}^{\pm2,0}$ should be considered. During the second period of $t_{DQ}/2$ the process that yields $T_{3,\pm2}^{\pm2,0}$ and $T_{4,\pm2}^{\pm2,0}$ is reversed. By a suitable phase cycling of the two $\pi/2$ pulses on the ^2H nucleus, one selects the pathway (shown in Fig. 6) that transfers the tensors $T_{3,2}^{2,0}$ via $T_{3,-3}^{-2,-1} = T_{2,-2}(^2H_1)T_{1,-1}(^2H_2)$ to $T_{3,-2}^{-2,0}$ and eliminates the contribution of $T_{2,\pm2}(^2H)$ and $T_{4,\pm3}^{\pm2,\pm1} = T_{2,\pm2}(^2H_1)T_{2,\pm1}(^2H_2)$. Thus, one observes only deuterons that correlate with one another and are affected by quadrupolar interaction only to the second order.

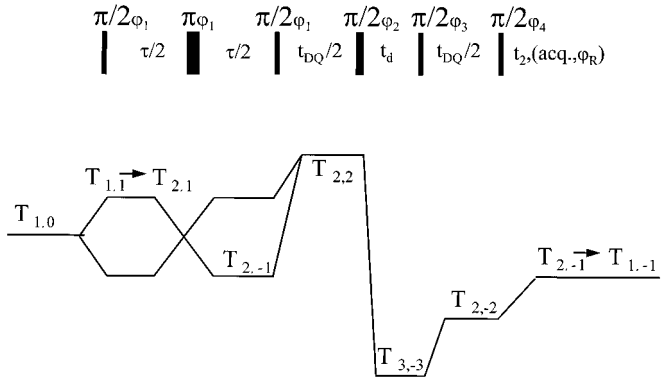

FIG. 6. A pulse sequence designed for the detection of homonuclear third-rank tensor $T_{3,-3}$, denoted as homonuclear triple-quantum filter (Hom-TQF). The phase cycling is $\varphi_1 = 0$, $\varphi_2 = j*\pi/10 + (k + m)*0$, $\varphi_4 = (j + m)*0 + k*\pi/2$, $\varphi_R = j*\pi/2 - (k + m)*\pi/2$, $j = 0, 1, \cdots, 19$ and k, $m = 0, 1, 2, 3$. The asterisk denotes multiplication.

By selecting a constant value for t_{DQ} and τ, and varying the time interval, t_d, it is possible to obtain a 2D map. The selection of the tensor $T_{3,-3}^{-2,-1}$ during the period t_d makes the FID detection phase sensitive also in the t_d dimension. The tensor $T_{3,-3}^{-2,-1}$ during t_d and $T_{1,-1}$ during t_2 are governed by the quadrupolar interaction (*13, 21*); i.e., the Fourier transformation of the FID consists of two peaks in both dimensions f_d and f_2. However, in the f_d dimension, the peaks have the same phase (because $T_{3,-3}^{-2,-1}$ is present at $t_d = 0$) while in the f_2 dimension the two peaks are in antiphase to one another (due to the fact that for $t_2 = 0$ one has predominantly the tensor $T_{2,-1}(^2H)$ which then evolves to the detectable tensor $T_{1,-1}$ (*13, 18*)). From the discussion above it is possible to conclude that obtaining a 2D spectrum by the Hom-TQF pulse sequence (Fig. 6) is clear evidence for dipolar interaction between two deuterons.

e. The Relaxation Effects Caused by the Modulation of the Dipolar Interactions by Reorientation

The anisotropic reorientation motion has two significant effects. One is the first-order average of the quadrupolar and dipolar Hamiltonians resulting in residual values. The other effect of the reorientation motion is the second-order relaxation. Two cases are of interest in the current work. The first is the relaxation of double-quantum transitions of the deuterons, caused by the dipolar interaction with protons. The second is the relaxation of single-quantum transitions of the protons, caused by the dipolar interaction with other protons. In the first case, under the assumption that $2D\tau_C < 1$ (D is the dipolar interaction and τ_C is the reorientation correlation time of the ^{1}H–^{2}H internuclear vector), the following expressions for the DQ relaxation time (T_{DQ}) were obtained (*15, 22*):

$$\frac{1}{T_{DQ}} = \frac{2}{15} D^2 S(S+1)[8J(0) + J(\omega_I - \omega_S) + 12J(\omega_S) + 3J(\omega_I) + 6J(\omega_I + \omega_S)]$$

$$D^2 = \frac{\hbar^2 \gamma_S^2 \gamma_I^2}{r^6}. \qquad [19]$$

γ_I and γ_S are the gyromagnetic ratios of ^{2}H and ^{1}H nuclei, respectively. For very slow isotropic motions ($\omega_0\tau_C \gg 1$) and dipolar interaction with protons, T_{DQ} simplifies to

$$\frac{1}{T_{DQ}} = \frac{4}{5} D^2 \tau_C = \frac{4\hbar^2 \gamma_S^2 \gamma_I^2}{5r^6} \tau_C. \qquad [20]$$

For single-quantum relaxation due to homonuclear dipolar interaction (*23*),

$$\frac{1}{T_2} = \frac{1}{5} D^2 I(I+1)[3J(0) + 5J(\omega_I) + 2J(2\omega_I)]$$

$$D^2 = \frac{\hbar^2 \gamma_I^4}{r^6} \qquad [21]$$

and for very slow isotropic motions ($\omega_0\tau_C \gg 1$) $1/T_2$ of protons simplifies to

$$\frac{1}{T_2} = \frac{9}{20} D^2 \tau_C = \frac{9\hbar^2 \gamma_I^4}{20r^6} \tau_C. \qquad [22]$$

EXPERIMENTAL

Fresh bovine Achilles tendons were obtained from a slaughter house. They were cooled immediately in ice and, within a couple of hours, immersed in solutions composed of various ratios of H_2O and D_2O at 4°C for 36 h. NMR measurements were taken on a Bruker 360AMX WB and a 500ARX with magnetic field strengths of 8.46 and 11.74 T, respectively, using 10-mm probes.

TABLE 1
Proton Exchange Rate and ^{1}H–^{1}H Residual Dipolar Interaction as a Function of Temperature

Temperature, °C	1.5	24	41
k, s^{-1} [a]	1750	3500	6000
$\delta/2\pi = 3\omega_{^1H-^1H}/2\pi$, Hz[a]	900	900	830
δ/k	3.2	1.6	0.94

[a] The experimental error resulting from S/N and biological variability is ±20% for k and ±10% for δ.

RESULTS AND DISCUSSION

Measurements of the Effect of the Residual ^{1}H–^{1}H Interaction on the ^{1}H Spectrum

Measurements of the ^{1}H–^{1}H dipolar interaction were taken on bovine Achilles tendons immersed in solutions of 93% H_2O and 7% D_2O at several temperatures. Two types of measurements were taken. One is the conventional DQF (Fig. 1; see Section a.III) and the second is IP-DQF (Fig. 2; see Section a.III). For the former pulse sequence, we obtained spectra consisting of two peaks with opposite phases, similar to previously reported results (*19*). The spectral peak intensities were measured as a function of the creation time τ. The results at temperatures of 1.5 and 24°C fitted well the expression given in Eq. [3a] while those measured at a temperature of 41°C fitted Eq. [3c]. The results of the fit are summarized in Table 1. The value of the proton exchange rate, k obtained at a temperature of 24°C, 3400 s^{-1} (Table 1), is similar to that found in pure water at the same temperature and a pH of 6.4 (*24, 25*). As could be expected, the splitting, δ (Eq. [3]), is temperature independent while the proton exchange rate, k, changes by more than a factor of 3. The ratio δ/k varies from 3.2 to 0.94. While for $\delta/k = 3.2$ a well-resolved spectrum is obtained, no splitting is observed for the ratio of 0.94. This effect is clearly demonstrated in the results shown in Fig. 7, where the pulse sequence IP-DQF was used. At 1.5°C, the spectrum consists of well-resolved peaks which, at higher temperatures, broaden and eventually coalesce. The peak intensity of the IP-DQF (as well as the DQF) spectra declined (Fig. 7) with increasing temperature. This observation is consistent with theory that predicts $1/k^2$ (Eqs. [7] and [10]) dependence on the proton exchange rate. It is important to note that, in order to ascertain whether a pair of peaks are well resolved in the conventional DQF and the IP-DQF experiments (Figs. 1 and 2, respectively) one has to select dispersive and absorptive phases, respectively. A spectrum presented in a dispersive mode decays off as $1/\omega$, while a spectrum displayed in an absorptive mode falls off

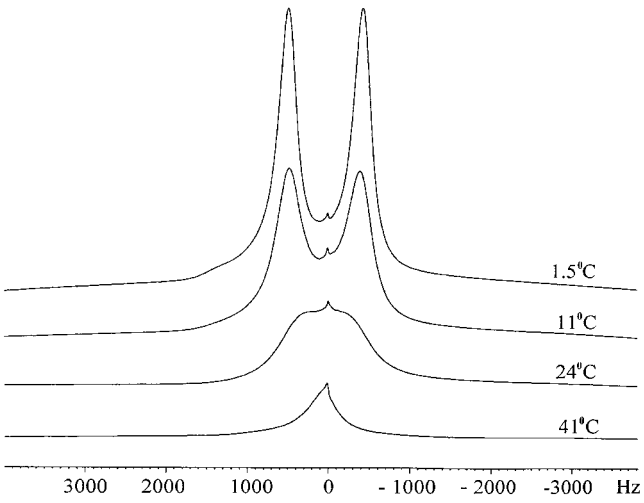

FIG. 7. IP-DQF (Fig. 2) spectra of a bovine Achilles tendon immersed in a solution of 93% H_2O and 7% D_2O given as a function of temperature. The creation time τ is 560 μs. The number of scans was 64. An exponential broadening of 5 Hz was used.

as $1/\omega^2$. Thus, the resolution of the IP-DQF experiment is better than that of the conventional DQF (graphical representation of dependence of the resolution of the conventional DQF spectra on the splitting, δ, can be found elsewhere (*12*)). In order to verify that the main cause for the above changes in the ^1H spectra is modulation of ^1H–^1H dipolar interaction by the proton exchange, we have repeated the above measurements for ^2H for the following reason: as the splitting of the ^2H nuclei is caused by quadrupolar interaction, it is not expected to be modulated by proton exchange in systems with small variations of the electric field gradient. Indeed, over the whole range of temperatures, no change in the splitting and only minor changes in the lineswidths have been noticed. Any significant effect of the 7% D_2O on the ^1H spectra could be ruled out by the fact that ^2H decoupling did not significantly change the ^1H spectrum.

Measurements of the Residual ^1H–^2H Interaction Using ^1H and ^2H Detection

Measurements of the ^1H–^2H dipolar interaction were taken on bovine Achilles tendons immersed in solutions of 93% H_2O and 7% D_2O or 7% H_2O and 93% D_2O at several temperatures. Four types of measurements were carried out: DQRE (Fig. 4; see Section c.III), Het-TQF (Fig. 5; see Section c.III) with ^2H detection, and the two pulse sequences Inv-XSQ and Inv-XDQ where the ^1H is detected (Fig. 3; see Section b.II). Control experiments were carried out for the latter three experiments by setting the rf frequency of the pulses applied to the nuclei which are not detected at off resonance. As expected, the control experiments yielded no FID.

For the 93% H_2O and 7% D_2O samples, 96% of the deuterons are found in the form of HDO molecules and thus the ^1H–^2H dipolar interaction dominates the results of the DQRE and Het-TQF experiments. Similarly in the 7% H_2O and 93% D_2O solution, most of the water protons are present in the HDO molecules. Thus, the results of the measurements that use the Inv-XSQ and Inv-XDQ pulse sequences are dominated by the ^1H–^2H dipolar interaction. The DQRE and Het-TQF pulse sequences gave spectra that consisted of two peaks with opposite phases (peaks with poor resolution and small intensity in the center of the ^2H spectra had little effect on the current work analysis and thus were ignored). As for the IP-DQF experiment of protons Het-TQF peak intensities increased with decreased temperature due to the $1/k^2$ dependence on the hydrogen exchange rate. The spectral peak intensities of the Het-TQF experiment were measured as a function of the evolution time t_{DQ}. The results of the Het-TQF experiment at a temperature of 1.5°C were successfully fitted, using a nonlinear mean squares method, to Eq. [17a] while, at 24 and 41°C, the results were fitted to Eq. [17c]. The results of the fit are summarized in Table 2 and an example of the experimental results along with the fitted curve (Eq. [17c]) is given in Fig. 8. As could be expected, the splitting, δ (Eq. [3]), is temperature independent while the proton exchange rate, k, changes by at least a factor of 3. The ratio δ/k varies from 1.25 to 0.22. These values were smaller than those obtained from the ^1H DQF (as expected) as the ^1H–^2H dipolar interaction is smaller than that of the ^1H–^1H interaction. As seen from Tables 1 and 2, the ratio between the splittings, caused by ^1H–^2H and ^1H–^1H dipolar interactions, is about 0.21 which is in agreement with the theoretical value of 0.205 (Section c.I). The values obtained for the proton exchange rates from the Het-TQF experiment (Table 2) are smaller than those obtained from the ^1H DQF experiment (Table 1). This difference can be partially attributed to the proton–deuteron isotope effect since part of the hydrogen exchange process that affects the Het-TQF experiment is a proton–deuteron exchange. For comparison one can site the ratio between proton exchange rate in H_2O to that of deuterium in D_2O to be 3.8 at 24°C and pH 6.4 (*25*). The isotope effect in the Het-TQF experiment is expected to be less than half of that value, in agreement with the experimental result of 1.5 at 24°C (Tables 1 and 2). Further experimental evidence that

TABLE 2
Proton Exchange Rate and ^1H–^2H Residual Dipolar Interaction as a Function of Temperature

Temperature, °C	1.5[a]	24[a]	41[b]
k, s^{-1}	700	2400	8000
$\delta/2\pi = 4\omega_{^1H-^2H}/2\pi$, Hz	190	190	280
δ/k	1.25	0.57	0.22

[a] The experimental error resulting from S/N and biological variability is $\pm$20% for k and $\pm$10% for δ.

[b] The experimental error resulting from S/N and biological variability is $\pm$40% for k and $\pm$20% for δ.

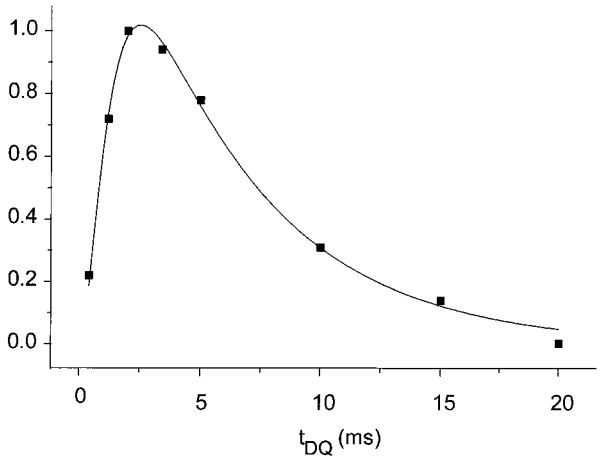

FIG. 8. Experimental result of the Het-TQF pulse sequence (Fig. 5), applied to a bovine Achilles tendon immersed in a solution of 93% H_2O and 7% D_2O at 24°C. A creation time of $\tau = 0.2$ ms was used in order to optimize S/N. Points are the experimental data and the full line was obtained by fitting to Eq. [17c] (the fast exchange case).

supports the analysis of the results of the Het-TQF experiments is provided by the orientation dependence of the results of these experiments. As suggested by Eq. [17], changing the sample orientation from parallel to perpendicular to the magnetic field should cause a decline of the spectrum intensity. However, part of the reduction of the intensity stems also from the reduction of the quadrupolar interaction for the perpendicular orientation. This difficulty can be resolved by comparing the expressions of the Het-TQF with those of DQRE. As can be seen from Eqs. [15] and [17], the two experiments have the same dependence on the quadrupolar interaction, given by $f_{12}^{q}(\tau, t_2)$. Thus, by normalizing the Het-TQF spectra by the spectrum obtained in the DQRE experiment when t_{DQ} (Fig. 4) is very short, one obtains $U_3^2(t_{DQ}/2)$ (Eq. [17]) where the effect of the quadrupolar interaction is eliminated and the effect of the dipolar interaction is retained. Normalized Het-TQF spectra for the samples oriented perpendicular to the magnetic field were simulated using the values for the hydrogen exchange rate and the dipolar splitting given in Table 2. The ratio between the largest peak intensities of the parallel and perpendicular orientations was calculated to be 2.3. Experimentally, for samples at temperature of 1.5°C, a value of 2.7 was found.

The ^{1}H–^{2}H dipolar interaction and proton exchange rate can also be obtained from the dependence of signal intensity on t_{DQ} in the DQRE experiment (Fig. 4 and Eq. [15]). As can be seen from Eq. [15], for very slow exchange, the FID is a single exponential with a decay rate of $k/2$. In the intermediate exchange regime, where $k \geq 4\omega_{^1H-^2H}$, the FID depends on both k and $\omega_{^1H-^2H}$. Although the fitting of experimental data to Eq. [15] is less reliable, compared to the Het-TQF experiment, one obtains, at 1.5°C, 550 ± 90 s^{-1} and 210 ± 30 Hz for the proton exchange rate and the ^{1}H–^{2}H dipolar splitting, respectively. These results compared favorably with the results obtained by the Het-TQF experiment (Table 2). In the fast exchange limit ($k > 16\omega_{^1H-^2H}$, Eq.[15c]), the FID decays as a single exponential with a decay rate of $1/T_{DQ} = 4\omega^2_{^1H-^2H}/k$. Therefore $\omega_{^1H-^2H}$ and k cannot be independently determined. However, on the basis of $\omega_{^1H-^2H}$ and k determined by the Het-TQF experiments at 24°C (Table 2), it was possible to calculate $1/T_{DQ}$. The values obtained are 6.4 ± 1.2 and 15 ± 3 ms for parallel and perpendicular orientations, respectively. They are in agreement with the DQRE experimental values of 6.4 ± 0.7 and 16 ± 2.

A method for independently verifying that T_{DQ} (Eq. [15]) is dominated by the ^{1}H–^{2}H dipolar interaction is to measure it by DQRE (Fig. 4) along with proton decoupling during the period t_{DQ}. Indeed, the decoupling caused the T_{DQ} to be lengthened from 6.4 ms at 24°C and 3.5 ms at 1.5°C to 43 ms at both temperatures. While the results at 24 and at 1.5°C with proton decoupling behaved as single exponentials, the results at 1.5°C without decoupling only approximated it. These results are clear evidence for the effect of the ^{1}H–^{2}H dipolar interaction.

As explained at the beginning of the current section, the ^{1}H–^{2}H dipolar interaction can be measured with detection of the ^{1}H FID of samples containing 7% H_2O and 93% D_2O. In Fig. 9, a spectrum measured by the pulse sequence Inv-XSQ at a temperature of 1.5°C is given. Two peaks in opposite phases and separated by 175 Hz are evident. In the Inv-XDQ experiment (not shown) three peaks are obtained. The two outermost peaks were separated by 200 Hz and had the same phase, opposite to that of the central peak (for theoretical details see Section b.II). The two outermost peaks of the ^{1}H single pulse (not shown) and IP-DQF spectra (separated by 950 ± 50 Hz, Fig. 7) are missing in both Inv-XSQ and Inv-XDQ experiments, indicating that they are a result of the ^{1}H–^{1}H dipolar interaction. On the basis of Eqs. [1], [11], and [12], one expects the ratios between the splitting in the ^{1}H DQF, Inv-XSQ, Het-TQF, and Inv-XDQ to be $3\omega_{^1H-^1H}$: $4\omega_{^1H-^2H}$: $4\omega_{^1H-^2H}$: $4\omega_{^1H-^2H}$,

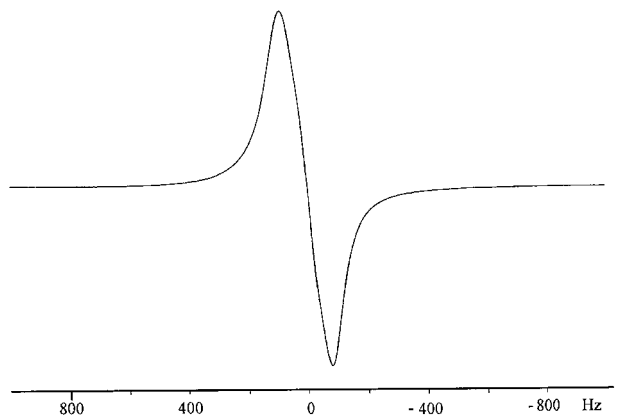

FIG. 9. An Inv-SQX (Fig. 3) spectrum of a bovine Achilles tendon immersed in a solution of 7% H_2O and 93% D_2O at 1.5°C. A creation time of $\tau = 0.6$ ms was used. The number of scans was 32. An exponential broadening of 1 Hz was used. The observed splitting was 175 Hz.

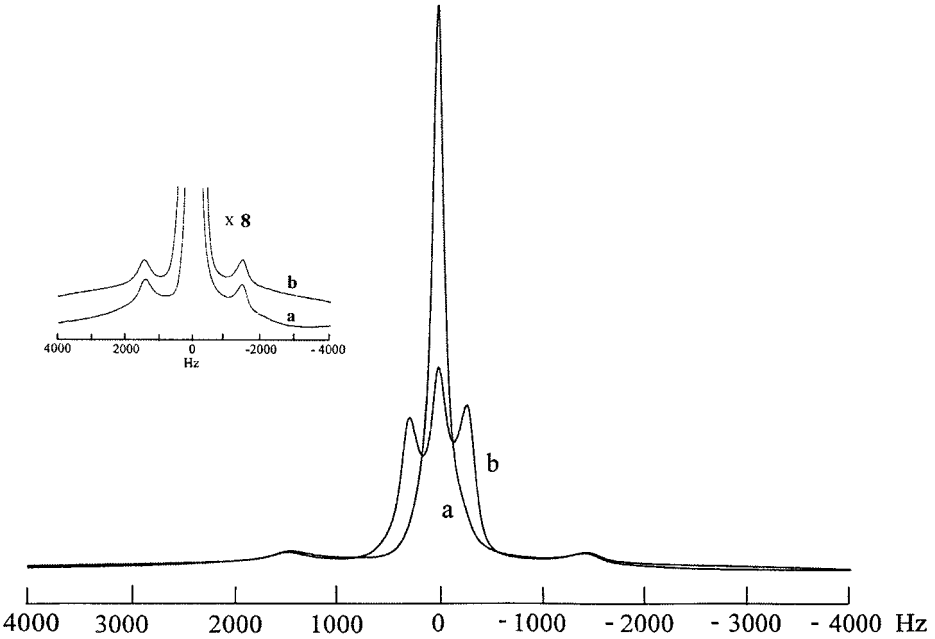

FIG. 10. A proton single-pulse spectrum of a bovine Achilles tendon immersed in a solution of 7% H_2O and 93% D_2O at a temperature of −14°C, (a) with and (b) without ^2H decoupling. Waltz-16 and cw decoupling were used with a radiofrequency magnetic field strength of 16 G. In the inset the splitting due to the H_2O molecules is shown in order to demonstrate the lack of effect when ^2H decoupling is applied. An exponential broadening of 10 Hz was applied.

i.e., 1:0.205:0.205:0.205. The experimental results on the basis of Fig. 9 and Tables 1 and 2 are 1:0.185:0.201:0.205, respectively. Thus, one can conclude that the splitting observed in the above experiments is due to ^1H–^1H and ^1H–^2H intramolecular interactions in the water molecules. A further demonstration of this conclusion is seen in the ^2H decoupling effect on the ^1H single-pulse spectrum of tendon in a solution of 93% D_2O and 7% H_2O at −14°C (Fig. 10). The spectrum consists of a doublet (split by 2.9 kHz) and a triplet with a splitting of 0.56 kHz between its outermost peaks. This spectrum is characteristic of H_2O and HDO water molecules in the same environment. Although the splittings at this temperature are considerably larger than those at 1.5°C, their ratio, 0.193, corresponds to the theoretical ratio of $4\omega_{^1H-^2H}/3\omega_{^1H-^1H} = 0.205$. This assignment is confirmed by the ^2H decoupling experiment. In this experiment the doublet is not affected while the triplet collapses. The latter effect becomes negligible at a temperature of 41°C as can be expected from the line narrowing caused by a fast proton exchange.

Measurements of the Residual ^2H–^2H Dipolar Interaction

Using the Hom-TQF pulse sequence (Fig. 6) a 2D spectrum for bovine Achilles tendon immersed in a saline solution of 100% D_2O was obtained (Fig. 11). To ensure that the observed FID originates from the tensors $T_{2,\pm2}(^2H)T_{1,0}(^2H)$ a DQ evolution time (t_{DQ}) of 10 ms was selected to be much longer than the lifetime of any single-quantum tensors. An estimate of 0.8 ms of this lifetime was obtained from the spectral linewidths of 400 Hz seen in the f_2 dimension of Fig. 11. Thus, it is concluded that during the period t_d one observes predominantly the evolution of the tensors

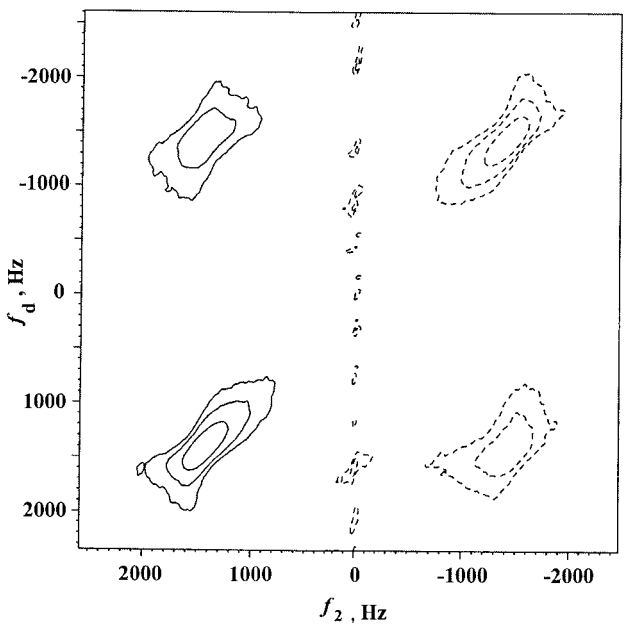

FIG. 11. A 2D ^2H spectrum of a bovine Achilles tendon immersed in a solution of 100% D_2O at 3°C. The spectrum was obtained by a suitable version (see text) of the Hom-TQF pulse sequence (Fig. 6). The creation time, τ, and DQ evolution time, t_{DQ}, were 0.2 and 10 ms, respectively. The number of scans was 80 and an exponential broadening of 40 Hz was used.

$T_{2,\pm2}(^2\mathrm{H})T_{1,\pm1}(^2\mathrm{H})$. For these tensors, inequivalent deuterons should give cross peaks in the 2D spectrum. The experimental results (Fig. 11) give a spectrum with the same quadrupolar splitting in the two dimensions. No cross peaks can be resolved. Thus we conclude that there is a significant intramolecular residual dipolar interaction between the deuterons of the D_2O molecules.

The Dependence of the Peak Intensities of the ^{1}H DQF and Inv-XSQ Experiments on the H/D Ratio

Supporting evidence for the identification of the interactions affecting the ^{1}H nuclei can be obtained from the dependence of the peak intensities on the ratio between the amounts of H_2O and D_2O in the solutions. We start our study at a temperature of 1.5°C, where the proton exchange rate is significantly smaller than the dipolar splitting. Under this condition, if the spectral lineshapes were determined by intramolecular dipolar interaction within the water molecules, the intensities in the ^{1}H DQF and Inv-XSQ experiments should be proportional to the amounts of H_2O and HDO molecules, respectively. Given a solution that was prepared by mixing H_2O and D_2O with ratio R, the fractions of H_2O, D_2O, and HDO in the solution are given by f_H^2, $(1 - f_H)^2$, and $2(1 - f_H) f_H$, where $f_H = R/(1 + R)$. If spectral lineshapes of the ^{1}H DQF experiment were determined by the ^{1}H–^{1}H dipolar interaction between a water proton and a protein proton, their intensities should depend linearly on the amount of H_2O. The tendon samples were immersed in two types of solutions. One consisted of 7% H_2O and 93% D_2O (denoted as solution a) and the second consisted of 93% H_2O and 7% D_2O (denoted as solution b). The final amounts of protons and deuterons in the samples were determined by integration of the single-pulse experiment spectra of the two nuclei. The experiments were repeated for two tendons with f_H increasing by a factor of 13 upon the replacement of solution a by solution b for one sample and by a factor of 11 for the second sample. Thus, if the dominant interaction was intramolecular, the intensities of the ^{1}H DQF spectra were expected to change by a factor of 169 or 121. In the case of intermolecular interactions with protein, the intensities of the ^{1}H DQF spectra were expected to change by a factor of 13 or 11. The ^{1}H DQF spectra consisted of a pair of peaks separated by 950 Hz and poorly resolved peaks in the center which are very small for the tendon immersed in solution a but have comparable intensities to the well-resolved lines for the tendon immersed in solution b. The intensities of the well-resolved peaks were changed for both samples by a factor of 150 upon the replacement of solution a by solution b, clearly indicating intramolecular dipolar interaction. Similar conclusions were reached by studying the dependence of the intensities of the spectra obtained by the Hom-TQF pulse sequence on the D_2O concentration at 1.5°C. Replacing solution a by b caused the intensities to increase by a factor larger than 100. Since the spectra obtained in the Inv-XSQ experiment are due to HDO molecules, whose concentrations are the same for solutions a and b, one expects the intensities of the spectra to be the same upon changing the solutions. In the experiments at 1.5°C, we get spectra that are weaker by a factor of 1.9 ± 0.3 for the 93% H_2O solutions. The deviation from a factor of 1 may be due to an effect of proton exchange which is sufficiently slow in order to have no effect on the ^{1}H–^{1}H dipolar splitting and is comparable to the ^{1}H–^{2}H splitting; i.e., the exchange process is in the intermediate regime. Indeed, preliminary results on collagen fibers show that the Inv-XSQ spectral intensity ratio between solutions a and b vary from 1.4 at temperature of −14°C to about 60 at 41°C. Thus, the intensity ratios are strongly dependent on the proton exchange when it is outside the slow exchange regime. For the bovine Achilles tendon, raising the temperature from 1.5 to 24°C changed the intensity ratio from 150 to 120. The increased deviation from the theoretical ratio of 169 is probably due to passage from the slow exchange regime into the intermediate regime.

CONCLUSIONS

The lineshape of the proton NMR of an excised bovine Achilles tendon is determined by the ^{1}H–^{1}H dipolar interaction. At low temperatures this interaction results in a splitting which coalesces above room temperature due to proton exchange. It is shown in the present work that both the spectral splitting and the intensity of the ^{1}H DQF signal are very sensitive to proton exchange. Moreover, one can obtain the dipolar splitting and exchange rate even for the fast exchange situation where they are inseparable by other methods. However, the MQF techniques are mostly useful for tissues where the residual dipolar interaction is not significantly smaller than the proton exchange rate.

Measurements of ^{1}H–^{2}H and ^{2}H–^{2}H dipolar interactions in addition to the ^{1}H–^{1}H interaction lead to the conclusion that the dipolar interaction is intramolecular, i.e., between the two water protons.

It is demonstrated that the dynamics of the double-quantum coherence of deuterons is dominated by dipolar interactions with protons, leading to the formation of the heteronuclear triple-quantum tensor (the Het-TQF experiment) and to DQ relaxation (the DQRE experiment). Similarly to the ^{1}H DQF experiment the Het-TQF experiment yields the hydrogen exchange rates and dipolar splitting.

Theoretical calculations demonstrate that in the fast exchange limit the relaxation times of the single-quantum coherence of the ^{1}H nucleus and of the ^{2}H double-quantum coherence depend on the square of the splitting caused by the intramolecular dipolar interaction with the proton in the same water molecule.

APPENDIX

a. General Equations

The density matrix equation of motion in the Liouville space is given by (*18, 26*)

$$\frac{d}{dt}\rho_p = A\rho_p\,, \qquad [A1]$$

where p is the coherence under consideration. A is a matrix representation of the superoperator $-i(H)^X O$ defined by $-i(H)^X O = -i[H, O]$. In the current work we consider only the effect of the secular part of the residual dipolar Hamiltonian H,

$$H = \alpha\omega_D(\theta)I_{z1}I_{z2}\,, \qquad [A2]$$

where $\alpha = 3, 2$ for the homonuclear ^{1}H–^{1}H and the heteronuclear ^{1}H–^{2}H dipolar interactions, respectively. D signifies the same interactions, i.e., either interactions between two protons or between a proton and a deuteron. The dependence of the dipolar interactions, $\omega_D(\theta)$, on the angle, θ, between the director axis (in the current work the cylindrical symmetry axis of the tissue) and the magnetic field is given by

$$\omega(\theta) = \omega_D^{loc}(3\cos^2\theta - 1)/2, \qquad [A3]$$

where ω_D^{loc} depends on the specific interacting nuclei, and for each particular case an expression is given in the text. The formal solution of Eq. [A1] is given by

$$\rho(t) = e^{At}\rho(0) = \tilde{U}(t)\rho(0), \qquad [A4]$$

where $\tilde{U}(t)$ is to be denoted as the evolution matrix.

b. The Effect of ^{1}H–^{1}H Residual Dipolar Interactions on $T_{1,\pm1}$ Tensors of the Protons in the Absence of Hydrogen Exchange

The representation of the matrix A of the single-quantum coherence, in a basis that consists of the eigenvectors of the ^{1}H–^{1}H homonuclear dipolar interaction, is given by (for convenience the eigenvectors are expressed in terms of the normalized spherical tensors $T_{1,\pm1}$ and $T_{2,\pm1}$)

$$A = \begin{pmatrix} T_{1,\pm1} - T_{2,\pm1} & T_{1,\pm1} + T_{2,\pm1} \\ \pm i\,\frac{3}{2}\omega_{^1\mathrm{H}-^1\mathrm{H}}(\theta) & \\ & \mp i\,\frac{3}{2}\omega_{^1\mathrm{H}-^1\mathrm{H}}(\theta) \end{pmatrix}. \qquad [A5]$$

The evolution matrix $\tilde{U}(t)$ is readily obtained from Eqs. [A4] and [A5]. However, for analysis of the experimental results it is convenient to use the normalized spherical tensor basis, $T_{1,\pm1}$ and $T_{2,\pm1}$, instead of the single element basis. The change of the bases is done by the similarity transformation

$$U(t) = T\tilde{U}(t)T^{-1}, \qquad [A6]$$

where T is given by

$$T = \frac{\sqrt{2}}{2}\begin{pmatrix} 1 & 1 \\ -1 & 1 \end{pmatrix}. \qquad [A7]$$

The resulting evolution matrix, U, is

$$U = \begin{pmatrix} T_{1,\pm1} & T_{2,\pm1} \\ \cos\frac{3}{2}\omega_{^1\mathrm{H}-^1\mathrm{H}}(\theta)t & \mp i\sin\frac{3}{2}\omega_{^1\mathrm{H}-^1\mathrm{H}}(\theta)t \\ \mp i\sin\frac{3}{2}\omega_{^1\mathrm{H}-^1\mathrm{H}}(\theta)t & \cos\frac{3}{2}\omega_{^1\mathrm{H}-^1\mathrm{H}}(\theta)t \end{pmatrix}. \qquad [A8]$$

c. The Effect of ^{1}H–X Residual Dipolar Interactions on $T_{2I,p}$ Tensors of the X Nucleus in the Absence of Hydrogen Exchange

For consideration of the effect of heteronuclear dipolar interaction on the p (I is the spin of the X nucleus) quantum coherence of the X nucleus interacting with protons the matrix A (Eq. [A1]) is represented in the normalized basis operators $T_{2I,p}(\mathrm{X})|m\rangle\langle m|$ ($m = \pm\frac{1}{2}$),

$$A = \begin{pmatrix} T_{2I,p}(\mathrm{X})|-\tfrac{1}{2}\rangle\langle-\tfrac{1}{2}| & T_{2I,p}(\mathrm{X})|\tfrac{1}{2}\rangle\langle\tfrac{1}{2}| \\ ip\omega_{^1\mathrm{H}-^2\mathrm{H}}(\theta) & \\ & -ip\omega_{^1\mathrm{H}-^2\mathrm{H}}(\theta) \end{pmatrix}, \qquad [A9]$$

where $p = \pm 2m_I$ with $m_I = \frac{1}{2}, \ldots, I$ or $m_I = 1, \ldots, I$ for half-integer or integer nucleus spins. The evolution matrix $\tilde{U}(t)$ is readily obtained from Eqs. [A4] and [A9]. The representation of the evolution matrix in the normalized spherical tensor basis, i.e., $T_{2I,p}(\mathrm{X})T_{0,0}(^1\mathrm{H})$ and $T_{2I,p}(\mathrm{X})T_{1,0}(^1\mathrm{H})$, is obtained by carrying out the transformation in Eq. [A6]:

$$U = \begin{pmatrix} \frac{1}{\sqrt{2}}T_{2I,p}(\mathrm{X}) & T_{2I,p}(\mathrm{X})T_{1,0}(^1\mathrm{H}) \\ \cos p\omega_{^1\mathrm{H}-\mathrm{X}}t & -i\sin p\omega_{^1\mathrm{H}-\mathrm{X}}t \\ -i\sin p\omega_{^1\mathrm{H}-\mathrm{X}}t & \cos p\omega_{^1\mathrm{H}-\mathrm{X}}t \end{pmatrix}. \qquad [A10]$$

d. The Effect of the ^{1}H–^{2}H Residual Dipolar Interaction on $T_{1,\pm1}$ Tensors of the Protons in the Absence of Hydrogen Exchange

The representation of the matrix A (Eq. [A1]) in the normalized basis operators $T_{1,\pm1}|m\rangle\langle m|$ ($m = 0, \pm1$) is

$$A = \begin{pmatrix} T_{1,\pm1}|-1\rangle\langle-1| & T_{1,\pm1}|0\rangle\langle0| & T_{1,\pm1}|1\rangle\langle1| \\ \pm i2\omega_{^1\mathrm{H}-^2\mathrm{H}}(\theta) & & \\ & 0 & \\ & & \mp i2\omega_{^1\mathrm{H}-^2\mathrm{H}}(\theta) \end{pmatrix}. \qquad [A11]$$

Following the procedure described in previous sections one obtains the evolution matrix $\tilde{U}(t)$ by substituting Eq. [A11] into Eq. [A4]. Similarly to the treatments of the other dipolar interactions the evolution matrix is represented in a normalized spherical tensor basis $T_{0,0}$, $T_{1,0}$, and $T_{2,0}$. This is achieved by the similarity transformation given in Eq. [A6] with T given in Eq. [A12] (T is the $I = 1$ analog of the expression given in Eq. [A7] for $I = \frac{1}{2}$):

$$T = \begin{pmatrix} \frac{\sqrt{3}}{3} & \frac{\sqrt{3}}{3} & \frac{\sqrt{3}}{3} \\ \frac{\sqrt{2}}{2} & 0 & -\frac{\sqrt{2}}{2} \\ \frac{\sqrt{6}}{6} & -\frac{\sqrt{6}}{3} & \frac{\sqrt{6}}{6} \end{pmatrix}. \qquad [A12]$$

The results of the similarity transformation are shown in Eq. [11], in the text.

e. The Effect of Proton Exchange on MQF Spectra

To obtain expressions for the evolution matrix in the case of proton exchange we use the following model. The coherence that is studied is assumed to form a correlation with a proton in the α or β spin state. Thus a chemical exchange between equal populations is considered (*26*). This effect of spin exchange on proton single-quantum and deuteron double-quantum coherence can be described by the scheme

$$T_{l,p}S^{\mathrm{a}}_{m} \underset{k/2}{\overset{k/2}{\rightleftharpoons}} T_{l,p}S^{\mathrm{b}}_{-m}, \qquad [A13]$$

where $S^i_m = {}^i|m\rangle\langle m|^i$ are single-element operators ($m = \frac{1}{2}$ or $-\frac{1}{2}$) for the protons and i = a, b. The indices a and b represent the two protons that were interchanged. $T_{l,p}$ are the normalized spherical tensors of the observed nucleus. For deuterons $l = 2$ and $p = \pm 2$ while for the case of a proton–proton interaction a symmetric form of $T_{l,p}S^i_m$ is used, with $l = 1$ and $p = \pm 1$. In this basis the following expression is obtained for the matrix A (Eq. [A1]), redefined to include the effect of proton exchange,

$$A = \begin{array}{c} \begin{matrix} T_{1,p}S^{\mathrm{a}}_{-1/2} & T_{1,p}S^{\mathrm{b}}_{1/2} & T_{1,p}S^{\mathrm{a}}_{1/2} & T_{1,p}S^{\mathrm{b}}_{-1/2} \end{matrix} \\ \begin{pmatrix} (i\alpha p\omega_{\mathrm{D}} - k)/2 & k/2 & 0 & 0 \\ k/2 & -(i\alpha p\omega_{\mathrm{D}} + k)/2 & 0 & 0 \\ 0 & 0 & -(i\alpha p\omega_{\mathrm{D}} + k)/2 & k/2 \\ 0 & 0 & k/2 & (i\alpha p\omega_{\mathrm{D}} - k)/2 \end{pmatrix} \end{array}, \qquad [A14]$$

where $\alpha = 2$ and 3 for ^{1}H–^{2}H and ^{1}H–^{1}H dipolar interactions, respectively, and ω_{D} can be either $\omega_{^1\mathrm{H}-^1\mathrm{H}}$ or $\omega_{^1\mathrm{H}-^2\mathrm{H}}$. The evolution matrix, $\tilde{U}(t)$, is obtained readily from Eqs. [A4] and [A14]. In order to obtain expressions that can be used to analyze the experimental results the evolution matrix is presented in the spherical tensor basis, i.e., $T_{l,p}T^i_{0,0}, T_{l,p}T^i_{1,0}$ (i = a, b). The transformation between the two basis sets is given by the similarity transformation given in Eq. [A6], where T is given by

$$T = \frac{\sqrt{2}}{2}\begin{pmatrix} 1 & 0 & 1 & 0 \\ 0 & 1 & 0 & 1 \\ -1 & 0 & 1 & 0 \\ 0 & 1 & 0 & -1 \end{pmatrix}. \qquad [A15]$$

The expression in Eq. [A15] is an extension of the transformation shown in Eq. [A7] to the case of proton exchange. The expressions obtained on the basis of Eqs. [A14], [A4], and [A15] for ^{1}H–^{1}H and ^{1}H–^{2}H dipolar interactions are presented in Eq. [3] and [13] in the text, respectively.

ACKNOWLEDGMENT

This work was supported by a grant from the U.S.–Israel Binational Science Foundation.

REFERENCES

1. D. M. Freeman, G. Bergman, and G. Glover, *Magn. Reson. Med.* **37,** 72 (1997).
2. Y. Xia, T. Farquhar, N. Burton-Wurster, and G. Lurst, *J. Magn. Reson. Imaging* **7,** 887 (1997).
3. H. J. C. Berendsen, *J. Chem. Phys.* **36,** 3297 (1962).
4. C. Migchelson and H. J. C. Berendsen, *J. Chem. Phys.* **59,** 296 (1973).
5. G. D. Fullerton, L. Cameron, and V. A. Ord, *Radiology* **155,** 433 (1985).
6. S. Peto, P. Gilles, and V. P. Henri, *Biophys. J.* **57,** 71 (1990).
7. R. M. Henkelman, G. J. Stainz, J. K. Kim, and M. J. Bronskill, *Magn. Reson. Med.* **32,** 592 (1994).
8. G. Bodenhausen, R. L. Vold, and R. R. Vold, *J. Magn. Reson.* **37,** 93 (1980).
9. G. Jaccard, S. Wimperis, and G. Bodenhausen, *J. Chem. Phys.* **85,** 6282 (1986).
10. U. Eliav, H. Shinar, and G. Navon, *J. Magn. Reson.* **98,** 223 (1992).

11. I. Furo and B. Halle, *Mol. Phys.* **76,** 1169 (1992).
12. U. Eliav and G. Navon, *J. Magn. Reson. B* **103,** 19 (1994).
13. Y. Sharf, U. Eliav, H. Shinar, and G. Navon, *J. Magn. Reson. B* **107,** 60 (1995).
14. S. Vega and Y. Naor, *J. Chem. Phys.* **75,** 75 (1981).
15. U. Eliav and G. Navon, *J. Magn. Reson. A* **123,** 32 (1996).
16. U. Eliav and G. Navon, *J. Magn. Reson.* **130,** 63 (1998).
17. R. M. Brunne, E. Liepish, G. Otting, K. Wüthrich, and W. F. van Gunsteren, *J. Mol. Biol.* **231,** 1040 (1993).
18. U. Eliav and G. Navon, *J. Magn. Reson. A* **115,** 241 (1995).
19. L. Tsoref, H. Shinar, and G. Navon, *Magn. Reson. Med.* **39,** 11 (1998).
20. A. Minoretti, W. P. Aue, M. Reinhold, and R. R. Ernst, *J. Magn. Reson.* **40,** 175 (1980).
21. R. Poupko, R. L. Vold, and R. R. Vold, *J. Magn. Reson.* **34,** 67 (1979).
22. D. Petit, J.-P. Korb, A. Delville, J. Grandjean, and P. Laszlo, *J. Magn. Reson.* **96,** 252 (1992).
23. A. Abragam, "Principles of Nuclear Magnetism," Oxford Univ. Press, Oxford (1961).
24. S. Meiboom, *J. Chem. Phys.* **34,** 375 (1961).
25. D. L. Turner, *Mol. Phys.* **40,** 949 (1980).
26. J. H. Freed, G. V. Bruno, and C. F. Polnasek, *J. Phys. Chem.* **75,** 3386 (1971).